JOURNAL OF APPLIED ELECTROCHEMISTRY 23 (1993) 463–470

Liquid-phase mass transfer enhancement by gas evolution at inclined plates

M. SHIRKHANZADEH, M. AJERSCH, L. W. SHEMILT*

Department of Chemical Engineering, McMaster University, Hamilton, Ontario, Canada L8S 4K1

Received 20 August 1990; revised 16 October 1992

The limiting current technique has been employed to determine mass transfer coefficients at vertical and inclined plates with stirring by coplanar electrochemical oxygen evolution. Orientation of the plate has been varied from −45 (down-facing inclined position) to +45 (up-facing inclined position) at ten intervals. At a constant oxygen evolution rate, maximum mass transfer enhancement was achieved at down-facing inclined orientations where θ (the angle from vertical) is small. The inclination angle at which mass transfer attained its highest value depended on the oxygen evolution rate and is given by

$$\theta_{max} = a + 10.96 \log I_g$$

where I_g (mA) is the electrochemical current for the oxygen evolution.

For the range of the inclination angle, $0 \leqslant \theta \geqslant \theta_{max}$, the relationship between the mass transfer coefficient and θ can be represented by

$$K = K_o + aK_o(\sin \theta)^{0.3}$$

where K_o is the mass transfer coefficient at the vertical plate.

Notation

a	constant in Equations 3 and 4
A	cathode surface area, cm^2
b	constant in Equation 4
C_b	bulk concentration, $mol\,cm^{-3}$
d	microelectrode diameter, cm
D	diffusion coefficient, $cm^2\,s^{-1}$
F	Faraday constant
F_b	buoyancy force, $g\,cm\,s^{-2}$
$F_{b,P}$	component of the buoyancy force parallel to the cathode surface, $g\,cm\,s^{-2}$
$F_{b,N}$	component of the buoyancy force normal to the cathode surface, $g\,cm\,s^{-2}$
F_s	shear force, $g\,cm\,s^{-2}$
g	gravitational constant, $cm\,s^{-2}$
Gr	Grashof number, $Gr = (gL^3/v^2)(\Delta\rho/\rho)$
I_g	current for oxygen evolution, mA
I_L	limiting current, A
k	local mass transfer coefficient, $cm\,s^{-1}$
K	average mass transfer coefficient, $cm\,s^{-1}$
K_o	average mass transfer coefficient at vertical plate, $cm\,s^{-1}$
L	cathode length, cm
Sc	Schmidt number $= (\mu/\rho D)$
Sh	*Sherwood number* $= (KL/D)$
V	*fluid velocity,* $cm\,s^{-1}$
z	*number of electrons exchanged in electrode reaction*

Greek letters

ε	*void fraction*
μ	*viscosity,* $g\,cm\,s^{-1}$
$\bar{\rho}$	*average density of gas-liquid dispersion,* $g\,cm^{-3}$
ρ_g	*density of gas,* $g\,cm^{-3}$
ρ_L	*density of liquid,* $g\,cm^{-3}$
δ_b	*thickness of the bubble layer, cm*
θ	*angle from vertical, degrees*
θ_{max}	*the angle for maximum mass transfer, degrees*

1. Introduction

The study of mass transfer at gas-sparged electrodes is of great interest, particularly in the view of improving the rate of mass transfer in electrochemical reactors. In this respect considerable work has been undertaken to measure the effect of stirring gases on the rate of mass transfer in electrochemical cells. In some instances, the stirring gas has been introduced into the cell from an external source [1–3]. Other work has been aimed at exploiting the counter electrode gases in stirring the cell to save external stirring energy. Fouad *et al.* [4], investigated the effect of cathodic hydrogen bubbles on the rate of mass transfer at a vertical copper plate dissolving in phosphoric acid, and reported an increase in the rate of mass transfer. Mohanta and Fahidy [5] and Ettel *et al.* [6], using parallel-plate copper electrowinning cells, measured the effect of the anodically generated oxygen bubbles on the rate of mass transfer at the vertical cell cathode.

* To whom correspondence should be directed.

0021-891X

The enhancing effect of anodic oxygen bubbles on the rate of mass transfer at the cathode was found not to exceed 20% [5]. New electrochemical reactor designs have been proposed to make more efficient use of the counter electrode gases in enhancing the rate of mass transfer at the working electrode. In one design, a modification of the traditional parallel-plate cell was suggested with a number of cells arranged vertically so that the working electrode of each cell was preceded by a gas-evolving electrode [7]. Other geometries such as an array of horizontal cylinders [8], an array of closely packed screen and vertical cylinders [9–11] and a fixed bed of spheres [12] were also studied for the improvement of mass transfer rates. In all these arrangements, mass transfer was found to increase more efficiently than in the traditional parallel plate reactor with gas evolving counter electrodes. In the area of mass transfer at gas-sparged electrodes, most investigations have been carried out on vertical or horizontal electrodes. This includes the study of coplanar electrolytic gas evolution which formed part of the elegant work of Whitney and Tobias [13] using a vertical micromosaic electrode. Similarly Giron *et al.* [14] measured local mass transfer coefficients in a vertical flow cell where coplanar electrogenerated gas bubbles were imposed on the flow regime. Analysis of results was based on classical correlations for turbulent flow and demonstrated an analogy between mass and momentum transfer. For inclined electrode systems Ahmed and Sedahmed [15] studied the effect of counterelectrode production of oxygen on the rate of mass transfer at inclined electrodes facing downward. An increase over the natural convection value of up to 116% resulted from the oxygen bubble stirring effect. Correlations of their results took into account the effect of electrode separation and oxygen discharge rate as well as angle of inclination ranging from 30° to 90° from the

The object of the present work is to study the effect of inclination angles upon the enhancement of mass transfer at a cathode plate, stirred by the oxygen evolved at a coplanar anode placed upstream from the cathode. Average mass transfer coefficients have been determined from the limiting currents corresponding to copper deposition at the test electrode. By means of microelectrodes inserted into the test electrode, it has also been possible to determine the distribution of local mass transfer coefficients along the test electrode at different orientations. Experimental data have been analyzed on the basis of the hydrodynamic model [16] to account for the effect of inclination angles on the mass transfer rates.

2. Apparatus and measuring techniques

Figure 1(a) is a simplified diagram of the experimental set-up, illustrating the test electrode (cathode), the oxygen generator electrode, auxiliary electrodes and corresponding circuitry for generating oxygen bubbles and mass transfer measurements. The test was carried out in a rectangular glass tank having dimensions of

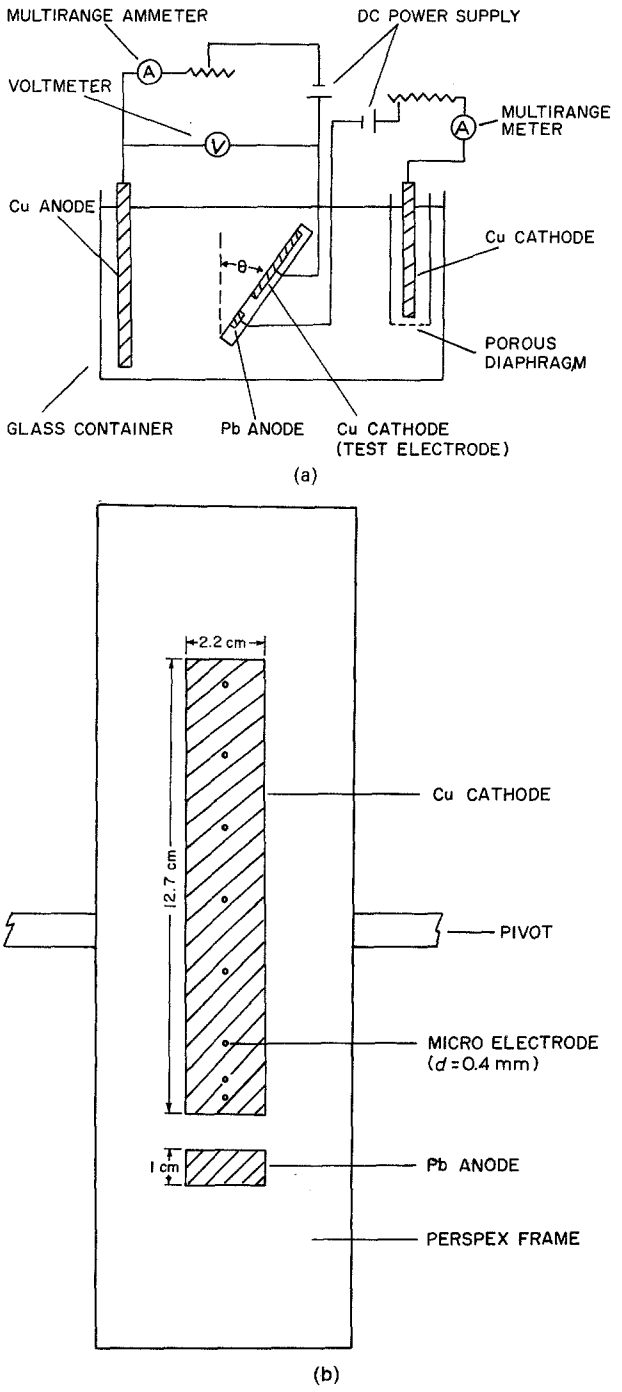

Fig. 1. (a) Schematic diagram of the experimental apparatus. (b) Schematic diagram of the test electrode.

60 cm × 30 cm × 30 cm (length × width × depth) which contained an electrolyte consisting of an aqueous solution of reagent grade cupric sulphate (0.05 M) and sulphuric acid (1.0 M) at room temperature (22–23° C). A schematic diagram of the test electrode (cathode), the generator electrode and the positions of the microelectrodes is given in Fig. 1(b). The test electrode was made of copper sheet 2.2 cm × 12.7 cm (width × height), with its active height ranging from 0.45 to 12.7 cm. The oxygen generator electrode was made of lead oxide (PbO_2) coated lead with an active surface area of 2.2 cm × 1 cm. Both the test electrode and the generator electrode were set into a thick Perspex frame with the test electrode being placed 1 cm from the upper edge of the generator electrode, the

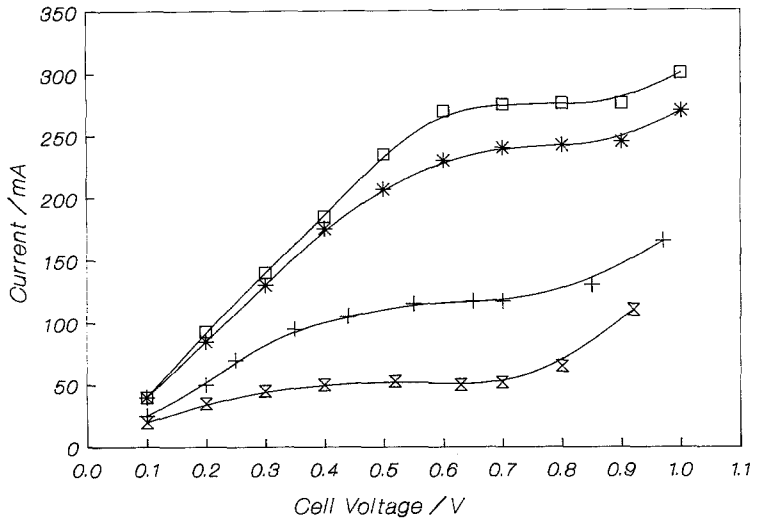

Fig. 2. Typical polarization curves obtained at different cathode orientations (L = 12.7 cm). I_g/mA, θ: (⧖) 0, 0°; (+) 500, +10°; (*) 500, 0°; (□) 500, −10°.

electrode surfaces being flush with the Perspex frame. The frame was attached to a horizontal pivot which allowed the whole deck in Fig. 1(b) to be oriented at any desired inclination angle, θ with respect to the vertical. Eight microelectrodes made of copper wire inserted into the test electrode served as mass transfer probes. The position of the microelectrodes are defined relative to the lower edge of the test electrode. Each probe was approximately 0.4 mm in diameter and was electrically insulated from the test electrode by a 0.05 mm thick insulating film. A standard 1.0 Ω shunt resistance was incorporated between each microelectrode and the test electrode.

As shown in Fig. 1(a), separate circuits were used for generating oxygen gas at the generator electrode and for mass transfer measurements at the test electrode. A copper sheet of 96 cm^2 was employed to serve as the cathode in conjunction with the generator electrode. To keep the bulk concentration of copper sulphate constant during the experiment, this cathode was placed in a cylindrical plastic tube which was closed at one end by a porous diaphragm. The rate of oxygen discharge was controlled by adjusting the current passing through the generator electrode. A large copper plate with a total active surface area of 500 cm^2 was also used to serve as the anode in conjunction with the test electrode. The relatively large surface area of the anode permitted its use as a reference electrode for mass transfer measurements. A d.c. power supply maintained the potential of the test electrode at limiting current conditions. Typical polarization curves are shown in Fig. 2.

Before each run, the test electrode was polished with fine emery paper, degreased with trichloroethylene and washed successively with alcohol and distilled water. Each run was begun by fixing the rate of oxygen discharge at the generator electrode. Then, with the potential of the test electrode held at limiting conditions, the orientation of the test electrode was varied at five degree intervals and the limiting current values recorded throughout the whole desired range of the inclination angles. Less than 2 min was usually sufficient to allow a steady state to be achieved following each orientation setting. The limiting current at each microelectrode was also determined by measuring the potential drop in the corresponding shunt resistance. This potential drop was sufficiently small that the microelectrodes and the test electrode can be considered to be at the same potential.

The overall mass transfer coefficient, K, was calculated from the well known equation:

$$K = \frac{I_L}{zFAC_b} \tag{1}$$

By measuring the limiting current at each microelectrode, the corresponding local mass transfer coefficient, k, was similarly calculated.

3. Results and discussion

The effect of the inclination angle, θ upon the overall mass transfer coefficient at various oxygen discharge rates, I_g, is shown in Fig. 3. The mass transfer coefficient in the absence of gas evolution (natural convection) is also presented in the lower part of the same figure. For natural convection (I_g = 0), the mass transfer coefficient has its minimum value at an inclination angle of θ = − 45° (downward-facing inclined position). As the angle tends toward the vertical the mass transfer rate slowly rises. Passing through the vertical, the value of the mass transfer coefficient is seen to increase and then level out at a maximum value corresponding to θ = 45° (upward-facing inclined position). Natural convection at inclined surfaces has been examined by several workers in the past including Sparrow and Husar [17], Patrick *et al.* [18] and Fouad and Ahmed [19]. When the data of these workers are compared with the data in this work, broadly similar trends in variation of K with θ are followed. According to Patrick *et al.* [18], attached flow conditions may be obtained for all downward-facing inclined orientations, the vertical position, and for upward-facing inclinations where θ is small. For attached boundary layer flow conditions, these authors correlated their

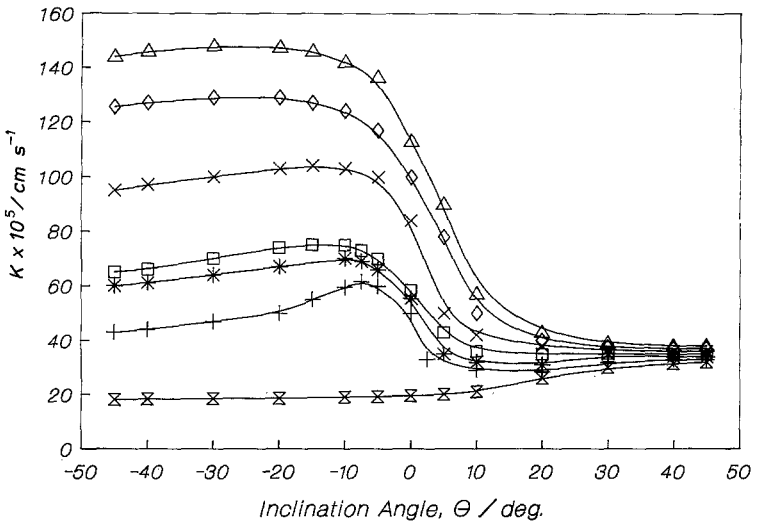

Fig. 3. Variations of mass transfer coefficients with inclination angles, at various oxygen discharge rates. I_g/mA: (⊗) 0; (+) 50; (*) 100; (□) 150; (×) 500; (◇) 1000; (△) 1600.

results by the equation:

$$Sh = 0.68(Sc\ Gr \cos\theta)^{0.25} \quad (2)$$

In the present work, the mass transfer coefficient, in the absence of gas evolution, shows, for all the downward-facing orientations, a linear dependence with $(\cos\theta)^{0.25}$ in agreement with Equation 2 for the attached boundary layer conditions. However, for small positive angles (upward-facing), the results do not follow Equation 2. Instead, for the range of positive angles a more complex dependence on θ is observed which is closely associated with the flow instability which arises at inclined upward-facing surfaces, including separation of the initially attached laminar boundary layer. In the present work, the onset of laminar-turbulent transition occurs at extremely small angles due to the large Rayleigh number involved (large electrode length).

For a constant oxygen discharge rate, the value of the mass transfer coefficient at a given value of θ may be compared with the corresponding value at the vertical position ($\theta = 0°$). As the inclination angle increases from the vertical position towards positive values, the mass transfer coefficients decline sharply at first (for $\theta < 10°$) and then slowly as the test electrode is further inclined (for $\theta > 10°$). The exceptions in this trend are the cases when the oxygen discharge rate is low ($I_g < 100$ mA). Under these circumstances, the mass transfer coefficient attains a minimum value at $\theta \approx 10°$. This is presumably because at such low rates of gas evolution, natural convection becomes the dominant factor at $\theta > 10°$. These observations are also consistent with the work of Whitney and Tobias [13] where they noted strong mass transfer enhancement for bubbles rising within the mass transfer boundary layer. For bubbles arising outside the boundary layer the effect on mass transfer was a steady laminar enhancement. In the case reported here small positive angles from the vertical (to the facing-upwards direction) would of course increasingly lead to bubbles outside the boundary layer. From Fig. 3 it can also be seen that at $\theta = +45°$ the mass transfer coefficient is little influenced by the I_g. Extrapolation of the data in Fig. 3 beyond 45° to 90° would similarly be expected to show an insignificant effect of the rate of gas generation (I_g) on the mass transfer coefficient (I_L). It can thus be claimed that almost the entire effect of rising gas bubbles on the mass transfer occurs when they are rising in close vicinity to the electrode surface, and that the corresponding limiting current is not significantly influenced by any possible electrical field interference.

Variations of mass transfer coefficients with θ at downward-facing inclined orientations reveal more interesting phenomena. For a given value of I_g, a rapid initial increase of the mass transfer coefficients is observed for small negative angles. As the inclination angle increases further, the mass transfer coefficient rises less rapidly before it reaches its maximum value, and then declines gradually as the inclination approaches $-45°$. The angle, θ_{max}, at which the mass transfer coefficients attains its maximum value depends strongly on the rate of oxygen discharge (I_g) (Fig. 4). For the range of the discharge rates studied here, the data may be represented by:

$$\theta_{max} = a + 10.96 \log I_g \quad (3)$$

where I_g is in mA.

Variations of mass transfer coefficients with I_g at the vertical position, at $\theta = -10°$ and at $\theta = +10°$ are shown in Fig. 5. The data for the vertical positions may be represented by:

$$K_o = aI_g^b \quad (4)$$

where $a = 1.26$ and $b = 0.255$, I_g is in mA and K_o is in cm s^{-1}. This value of the exponent b is consistent with the value of 0.269 obtained for a vertical plate electrode stirred by oxygen evolved at an upstream vertical anode flush with the cathode [7]. For gas evolving electrodes with no bubble coalescence, a value of 0.33 was obtained for the slope of $\log K/\log I_g$ by Janssen and Barendrecht [20] with the case assumed to be one of turbulent flow with natural convection.

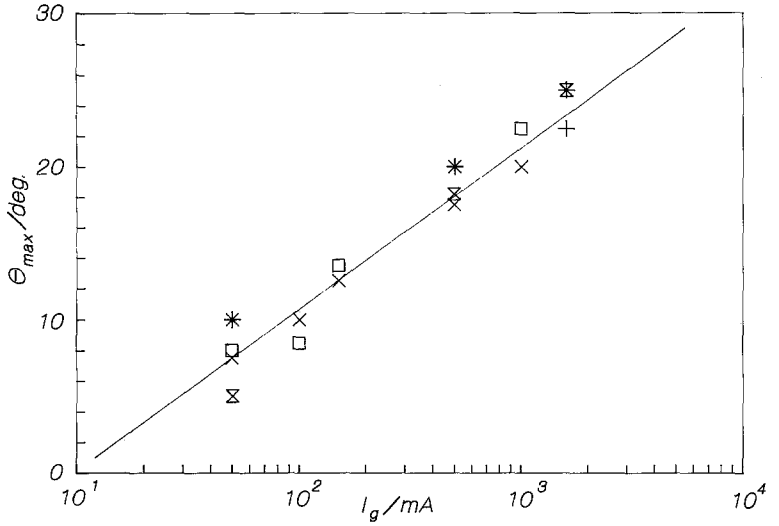

Fig. 4. Variations of θ_{max} with the oxygen discharge rates. L/cm: (⧖) 0.45; (+) 3.40; (*) 6.50; (□) 10.00; (×) 12.70.

Whitney and Tobias [13] also found this same 1/3 power dependence of mass transfer rate on bubble evolution rate for bubble streams rising outside the mass-transfer boundary layer. A possible approach to explain the relatively low $\log K/\log I_g$ slope in the present work is to consider the case as a laminar flow natural convection problem. A theoretical analysis in this case leads to a slope of $\log K$ against $\log I_g = 0.25$ [21] which is in close agreement with the present results. For $\theta = -10°$ and $\theta = +10°$, the data may also be correlated by equations similar to Equation 4 but with different values for the constant and only slightly different values for the exponent b.

The value of the mass transfer coefficients at θ_{max} for the range of I_g values shows a 24–32% increase over the corresponding values at the vertical position, and for the range of inclination angle $0 \leqslant \theta \leqslant \theta_{max}$ may be given by

$$K = K_o + aK_o(\sin\theta)^{0.30} \quad (5)$$

where K_o is the overall mass transfer coefficient at the vertical position ($\theta = 0$), given by Equation 4.

Figure 7 shows the effect of the electrode height on the average mass transfer coefficients for vertical and inclined orientations at $I_g = 50$ mA and $I_g = 1600$ mA. The slopes of $\log K$ against $\log L$ for the vertical and downward-facing inclinations are similar with values in the range of -0.215 to -0.242. These results are in fair agreement with the predictions based on the modified hydrodynamic model proposed by Janssen [22], where a laminar flow is assumed to be induced by rising bubbles along the electrode surface. According to this model, the average mass transfer coefficient is proportional to $L^{-0.25}$. The slope of $\log K$ against $\log L$ obtained in the present work is also in close agreement with the relationship holding for mass transfer under natural convection. The results however differ from those for the oxygen-evolving electrodes where the mass transfer coefficient is practically independent of L and thus supports the convection penetration model [20]. According to Fig. 7, the slope of $\log K$ against $\log L$ for upward-facing inclinations is higher than that for the vertical position since the bubble stream increasingly separates from the upper section of the test electrode with increasing L. The thickness of the hydrodynamic

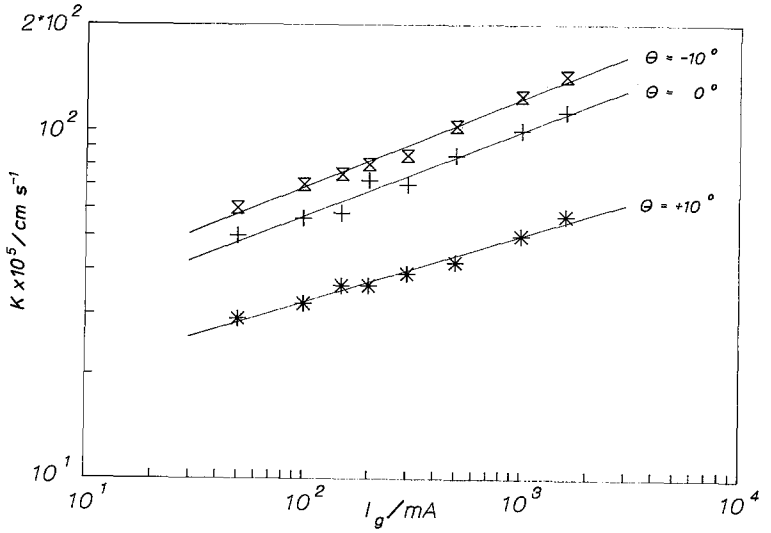

Fig. 5. Variations of mass transfer coefficients with oxygen discharge rates (L = 12.7 cm).

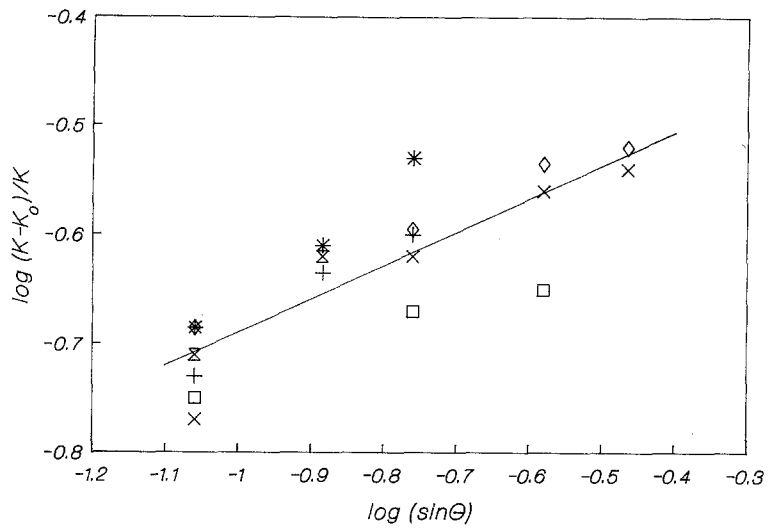

Fig. 6. Log $(K - K_0)/K_0$ against log sin θ for different oxygen discharge rates. I_g/mA: (⧖) 50; (+) 100; (*) 150; (□) 500; (×) 1000; (◇) 1600.

layer therefore also increases significantly along the electrode.

The variation of the mass transfer coefficients with the inclination angle, θ, as associated with the changes in the hydrodynamics of the liquid-gas dispersion in the vicinity of the test electrode fits the hydrodynamic model introduced by Janssen [23] and Janssen and Hoogland [24]. The experimental and analytical refinements introduced by Whitney and Tobias [13] provided data which resulted in their advocacy of a surface-penetration model for bubbles rising within the mass transfer boundary layer, and a rising cylinder model for the increased laminar flow along the electrode when bubble streams are effective outside the mass transfer boundary layer. The latter is essentially a form of hydrodynamic model which appears to be the most relevant model in interpreting the phenomenological aspects of this investigation. The hydrodynamic model is based on liquid flow arising due to the buoyant lift of the rising bubbles near the electrode. This is additive to the natural convection effect during the actual mass transfer arising from the concentration difference between the bulk electrolyte and the surface layer at the electrode with its accompanying buoyancy effect. The movement of the fluid adjacent to the electrode is largely governed by the average buoyancy force acting on the two-phase gas–liquid system. The average density of the system is

$$\bar{\rho} = \rho_g \varepsilon + (1 - \varepsilon)\rho_L \approx (1 - \varepsilon)\rho_L \qquad (6)$$

where the voidage ε is the fraction of the total volume occupied by the gas, and ρ_g and ρ_L are the densities of the gas and liquid, and the density of the gas is assumed negligible as compared to that of the liquid ($\rho_g \ll \rho_L$). The buoyancy force is given by the difference $\Delta\rho$ between the average density and the density of the liquid.

The upward force acting on a unit of volume of the two-phase system is given by:

$$F_b = g\Delta\rho = g(\rho_L - \bar{\rho}) = g\varepsilon\rho_L \qquad (7)$$

Because of the solution velocity gradient, a shear stress also acts downward on the solution element at

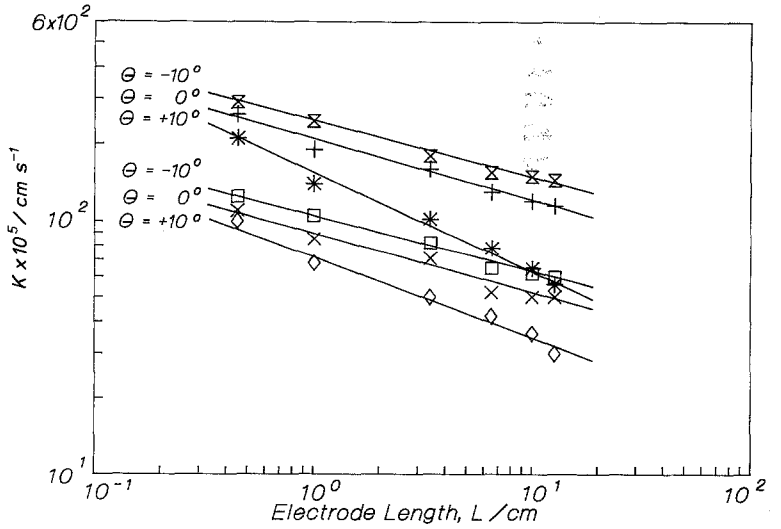

Fig. 7. Variations of mass transfer coefficients with the cathode lengths at different inclination angles. I_g/mA, θ: (⧖) 1600, −10°; (+) 1600, 0°; (□) 50, −10°; (*) 1600, +10°; (×) 50, 0°; (◇) 50, +10°.

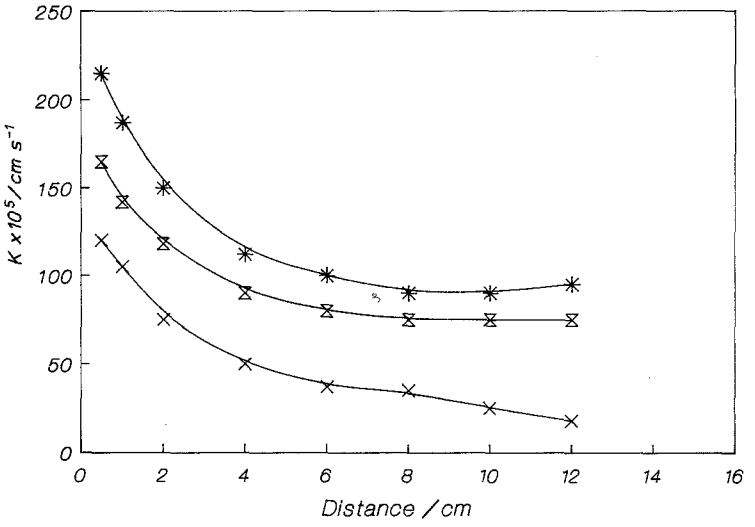

Fig. 8. Variations of k (local mass transfer coefficient) with position along the cathode at various inclination angles. For I_g = 500 mA, θ: (*) −10°; (⧖) 0°; (×) +10°.

the wall. This resulting shear force F_s is given by:

$$F_S = \mu\left(\frac{dV}{dy}\right)_w \tag{8}$$

where μ is the viscosity and (dV/dy) is the velocity gradient at the electrode wall.

At the vertical position (θ = 0°), a thin carpet of oxygen bubbles is formed next to the electrode surface. The trains of the bubbles are distributed uniformly across the width of the cathode plate. The thickness of the bubble layer, δ_b, and the size of the individual bubbles both increase with the oxygen discharge rate. This is accompanied by the acceleration of the velocity of the rising bubbles and enhancement of the mass transfer rate at the cathode surface. These phenomena were noted much earlier by Glas and Westwater [25] for vertical plates. For a given oxygen discharge rate, small departures from the vertical position towards positive angles results in an increase of δ_b since the horizontal projection of the anode surface increases with θ. The increase of the bubble layer thickness in turn results in the decrease of both the gas voidage fraction ε, and the buoyancy force acting on the gas–liquid dispersion, F_b. As θ increases further, the stream of bubbles increasingly separates from the cathode plate. All these factors favour a less intensified mass transfer rate at the cathode as indicated in Fig. 3 by a sharp drop of the mass transfer coefficients. A more interesting phenomenon is observed at the downward-facing orientations. At a constant oxygen discharge as the negative angle increases from its 0 value at the vertical position, there will be a compressive effect decreasing the thickness of the bubble layer, δ_b. The consequent higher buoyancy component normal to the electrode surface corresponds also to an increase in the velocity of the rising bubbles and a sharp enhancement of mass transfer (Fig. 3). For these downward-facing orientations, the trajectory of the ascending bubbles is parallel to and along the inclined cathode. The component of the buoyancy force acting on a unit value of the gas–liquid dispersion along the cathode is therefore given by:

$$F_{b,p} = g\varepsilon\rho_L \cos\theta \tag{9}$$

The component of the buoyancy force normal to the cathode surface is also given by:

$$F_{b,N} = g\varepsilon\rho_L \sin\theta \tag{10}$$

The normal component of the buoyancy force, $F_{b,N}$, pushes the bubbles against the cathode. As a result, at steady state conditions, a thin layer of gas–liquid dispersion is formed next to the cathode which has a relatively high gas voidage fraction, ε. Since ε increases significantly with θ, the net result at steady state is such that the force acting on the gas–liquid dispersion along the downward-facing cathode is indeed larger than the corresponding force at the vertical position (θ = 0°). This explains the observed enhancement of the mass transfer at the downward-facing cathode at $\theta < \theta_{max}$. For inclination angles greater than θ_{max}, coalescence of the ascending bubbles is clearly observed. As the inclination angle exceeds θ_{max}, the size of the individual bubbles increases while their number decreases considerably. This is accompanied by a gradual slow-down of the bubble velocity and a decline of the mass transfer coefficient (Fig. 3). This is closely related to the development of a significant friction force along the cathode plate since the large contact area between the individual bubbles and the cathode surface, together with the existence of a relatively large normal forces ($F_{b,N}$) play important roles in the development of this friction force.

To further understand the effect of inclination angles on mass transfer it is important to obtain quantitative information on local mass transfer coefficients at the cathode wall. Variations of local mass transfer coefficients (k) with distance (x) along the cathode plate for three different angles (θ = 0°, −10°, and +10°) and at I_g = 500 mA are presented in Fig. 8. For the vertical position (θ = 0°), the local mass transfer coefficients drop sharply at small distances from the leading edge of the cathode. However, at relatively large distances, a more or less constant value

of k is established. This trend is in agreement with the theory of the development of the boundary layer for laminar flow along a wall. A similar pattern is also observed for the negative inclination ($\theta = -10°$), although the value of k in this case at any location along the cathode is relatively higher than the corresponding value at the vertical position for the reasons given previously. For the positive inclination ($\theta = +10°$), k decreases continuously with distance as the bubbles in their upward motion become increasingly separated from the cathode plate, and their stirring effect therefore, diminishes.

4. Conclusions

This study has shown that the mass transfer at a gas-sparged plane cathode may be enhanced significantly at downward-facing inclined positions when θ (the inclination angle from the vertical) is kept small. The inclination angle, θ_{max}, at which the maximum enhancement of mass transfer occurs has been experimentally determined to be a function of the oxygen discharge rate. It has also been shown that the inclination angle has a similar effect on the local mass transfer coefficients at the cathode wall. The results demonstrate the importance of the proper choice of cathode orientations for the efficient operation of electrochemical reactors with gas-evolving counter electrodes.

Acknowledgement

The authors acknowledge with thanks the support of the Natural Science and Engineering Research Council of Canada.

References

[1] W. W. Harvey, M. R. Randlett and K. I. Bangeriskis. Presented at the 102nd Annual Meeting of the AIME, Chicago (1973).
[2] V. A. Ettel, A. S. Gendron and B. V. Tilak, *Metall. Trans.* **6B** (1975) 31.
[3] A. S. Gendron and V. A. Ettel, *Can. J. Chem Eng.* **53** (1975) 36.
[4] M. G. Fouad, F. N. Zein and M. I. Ismail, *Electrochim. Acta* **16** (1971) 1477.
[5] S. Mohanta and T. Z. Fahidy, *J. Appl. Electrochem.* 7 (1977) 235.
[6] V. A. Ettel, B. V. Tilak and A. S. Gendron, *J. Electrochem. Soc.* **121** (1974) 867.
[7] G. H. Sedahmed and L. W. Shemilt, *J. Appl. Electrochem.* **11** (1981) 537.
[8] *Idem, Can. J. Chem. Eng.* **60** (1982) 767.
[9] G. H. Sedahmed, *J. Appl. Electrochem.* **8** (1978) 339.
[10] *Idem, ibid.* **10** (1980) 351.
[11] *Idem, ibid.* **14** (1984) 693.
[12] G. H. Sedahmed, *Can. J. Chem. Eng.* **64** (1986) 75.
[13] G. M. Whitney and C. W. Tobias, *AIChEJ.* **34** (1988) 1981.
[14] F. Giron, G. Valentin, M. Lebouche and A. Storck, *J. Appl. Electrochem.* **15** (1985) 557.
[15] A. M. Ahmed and G. H. Sedahmed, *J. Electrochem. Soc.* **135** (1988) 2766.
[16] L. J. J. Janssen and J. G. Hoogland, *Electrochim. Acta* **15** (1970) 1013.
[17] E. M. Sparrow and R. B. Huser, *J. Fluid Mechanics* **37** (1969) 251.
[18] M. A. Patrick, A. A. Wragg and D. M. Pargeter, *Can. J. Chem. Eng.* **55** (1977) 432.
[19] M. G. Fouad and A. M. Ahmed, *Electrochim. Acta* **14** (1969) 651.
[20] L. J. J. Janssen and E. Barendrecht, *ibid.* **24** (1979) 693.
[21] G. H. Sedahmed and L. W. Shemilt, *J. Appl. Electrochem.* **14** (1984) 123.
[22] L. J. J. Janssen, *ibid.* **17** (1987) 1177.
[23] *Idem, Electrochim. Acta* **23** (1978) 81.
[24] L. J. J. Janssen and J. G. Hoogland, *ibid.* **18** (1973) 543.
[25] J. P. Glas and J. W. Westwater, *Int. J. Heat & Mass Trans.* 7 (1964) 1427.